

On the Estimation of Atomic Charges by the X-ray Method for Some Oxides and Silicates

BY SATOSHI SASAKI, KIYOSHI FUJINO,* YOSHIO TAKÉUCHI AND RYOICHI SADANAGA

Mineralogical Institute, Faculty of Science, University of Tokyo, Hongo, Tokyo 113, Japan

(Received 5 February 1980; accepted 18 May 1980)

Abstract

Based on accurate X-ray diffraction intensity data collected from spherically shaped single crystals, net atomic charges and electron density distributions have been studied for MnO , Mn_2SiO_4 , $\text{Mg}_2\text{Si}_2\text{O}_6$, $\text{LiAlSi}_2\text{O}_6$ and $\text{CaMgSi}_2\text{O}_6$. Examination of various procedures for determining atomic charges in a given structure has led to the conclusion that the following approach appears to be most reliable. (1) For cations: the number of electrons in the sphere of radius ER , *effective distribution radius*, which is defined according to the characteristics of radial distribution functions or difference-Fourier maps, is calculated. (2) For oxygen atoms: with the cation charges fixed at the values obtained from the above procedure and the total charge of the crystal constrained to be neutral, oxygen charges are estimated from least-squares refinements using atomic scattering factors. The final charges of atoms examined are less ionic than the corresponding formal ones: those of Li, O, Mg, Al, Si, Ca and Mn are respectively +0.7 (1), -1.1 to -1.5, +1.4 (1) to +1.8, +2.4 (1), +2.2 (1) to +2.6, +1.4 (2) and +1.2 (1) to +1.6 e. Residual electron densities between Si and O have been clearly observed in difference-Fourier maps after charge refinements for crystals of $\text{LiAlSi}_2\text{O}_6$, $\text{CaMgSi}_2\text{O}_6$ and $\text{Mg}_2\text{Si}_2\text{O}_6$.

Introduction

Basically, the charge of an atom is a concept used to characterize the state of ionization and is not measurable in a crystal. In studying the nature of the chemical bond crystal-chemically, however, the atomic charge may be discussed in terms of the electron density specifically associated with the atom in the crystal.

There are, in general, two approaches to estimate atomic charges by means of the X-ray diffraction method. One of them may be represented by the L -shell method as proposed by Stewart (1970). He showed

that the occupancy of electrons in a valence shell may be determined from X-ray structure factors by least-squares refinement. Coppens, Pautler & Griffin (1971) offered a refining technique in which positional and thermal parameters may be simultaneously varied together with occupancy parameters for valence electrons. Coppens, Guru Row, Leung, Stevens, Becker & Yang (1979) further extended the method by introducing a parameter κ as defined by $f(\sin \theta/\lambda\kappa)$. This parameter served to correct for an effect on f that may arise when atoms are brought to a crystalline state from a free state. This approach, however, involves the following difficulties. (1) Atomic scattering factors cannot be expressed as linear combinations of those for two different ionic states, especially in core and neutral states. (2) The difference in f between an atom in a crystalline state and one in a free state is not necessarily corrected for by the κ parameter. Sasaki, Fujino & Takéuchi (1979) in fact observed that the f 's experimentally determined for atoms in some mono-oxides of the NaCl type were not in accord with the form $f(\sin \theta/\lambda\kappa)$.

The other approach is to calculate, based on observed $F(hkl)$'s, the number of electrons in a sphere around a given atom. This method also involves the following difficulties. Firstly, the procedure requires extremely strict correction for termination errors in Fourier series; secondly, we must find an appropriate radius for the sphere. Studies of atomic charges along this line were made for simple crystal structures of the NaCl or CsCl type (e.g. Havighurst, 1927; Kurki-Suonio & Salmo, 1971; Vahbaselkä & Kurki-Suonio, 1975). In particular, Kurki-Suonio & Salmo (1971) discussed the procedures of determining atomic charges in detail and pointed out that this second approach gave more reliable results than that using f .

Using new sets of intensity data of MnO , Mn_2SiO_4 , $\text{Mg}_2\text{Si}_2\text{O}_6$, $\text{LiAlSi}_2\text{O}_6$ and $\text{CaMgSi}_2\text{O}_6$ and the results obtained from the study of electron density distribution of some mono-oxides (Sasaki *et al.*, 1979), we have made a thorough examination of the above two approaches to determine reliable atomic charges. The present paper describes the results obtained and presents an improved method together with its

* Present address: Department of Earth Sciences, Faculty of Science, Ehime University, Bunkyo-cho, Matsuyama 790, Japan.

applications to the moderately complex silicate structures. Preliminary communications on these procedures have been reported (Sasaki, Fujino, Takéuchi & Sadanaga, 1977, 1978).

Experimental

To test the validity of various procedures for estimating atomic charges by X-ray diffraction, five samples having different crystal structures were chosen: manganosite (MnO), tephroite (Mn_2SiO_4), ortho-enstatite ($\text{Mg}_2\text{Si}_2\text{O}_6$), α -spodumene ($\text{LiAlSi}_2\text{O}_6$) and diopside ($\text{CaMgSi}_2\text{O}_6$). The first three samples were synthesized respectively by the Bernoulli, Czochralski and lithium vanadomolybdate-flux methods, and the last two were natural crystals from Rumford, USA, and Mt Higashi-Akaishi, Japan. The crystal of Mn_2SiO_4 was pure within the analytical accuracy of EPMA, while a wet chemical analysis showed that MnO included a trace amount of Mn_2O_3 or MnO_4 . The $\text{Mg}_2\text{Si}_2\text{O}_6$ specimen contained 0.09 wt% Al_2O_3 , 0.08% TiO_2 , 0.16% ΣFeO , 0.17% Li_2O and 0.27% V_2O_5 ; $\text{LiAlSi}_2\text{O}_6$ contained 0.22 wt% Fe_2O_3 and 0.08% Na_2O ; $\text{CaMgSi}_2\text{O}_6$ contained 1.17 wt% Al_2O_3 , 2.46% ΣFeO and 0.48% Na_2O .

The cell dimensions were obtained from single-crystal diffractometry using graphite-monochromatized Mo $K\alpha$ radiation ($\lambda = 0.71069 \text{ \AA}$). In each case a crystal was ground to a spherical shape and

the ω - 2θ technique was used to collect, at room temperature, the intensity data up to $2\theta = 157^\circ$ (with parallel mode for $134 < 2\theta \leq 157^\circ$) for MnO, and up to $2\theta = 134^\circ$ with bisecting mode for the other samples. Three standard reflections used in each case were stable within 3% of integrated intensity during data collection. A set of 74 independent reflections of MnO was used for refinements after averaging all equivalent reflections measured (Sasaki *et al.*, 1979). The crystallographic data and experimental conditions are summarized in Table 1.

Each set of intensities was corrected for Lorentz and polarization factors (with program SYMT and PTPHI respectively for Syntex $P2_1$ and Philips PW1100 diffractometers), absorption, anomalous dispersion and isotropic extinction effects (Zachariasen, 1967; Coppens & Hamilton, 1970; Becker & Coppens, 1974). The atomic scattering factors for various ionic states were obtained mostly from *International Tables for X-ray Crystallography* (1974) and Fukamachi (1971). That for O^{2-} was provided by Tokonami (1965) and that for Si^{3+} from *International Tables for X-ray Crystallography* (1962). The values of the scattering factors were polynomially approximated, always fixing the original values, with a division of 0.01 \AA^{-1} in $\sin \theta/\lambda$. The anomalous dispersion terms for each atom were obtained from *International Tables for X-ray Crystallography* (1974). The crystal-structure refinement of $\text{LiAlSi}_2\text{O}_6$ has previously been carried out for the same crystal (Sasaki, 1976).

Table 1. *Crystal data and experimental conditions*

	MnO	$\text{LiAlSi}_2\text{O}_6^*$	$\text{CaMgSi}_2\text{O}_6$	$\text{Mg}_2\text{Si}_2\text{O}_6$	$\text{Mn}_2\text{SiO}_4^\dagger$
Space group	<i>Fm3m</i>	<i>C2/c</i>	<i>C2/c</i>	<i>Pbca</i>	<i>Pbnm</i>
Cell dimensions <i>a</i> (Å)	4.446 (1)	9.461 (2)	9.741 (1)	18.227 (4)	4.902 (1)
<i>b</i>		8.395 (1)	8.919 (2)	8.819 (2)	10.595 (2)
<i>c</i>		5.217 (1)	5.257 (1)	5.179 (1)	6.256 (1)
β (°)		110.09 (3)	105.97 (2)		
<i>V</i> (Å ³)	87.87 (4)	389.1 (2)	439.3 (2)	832.5 (3)	324.9 (1)
Chemical unit	4	4	4	8	4
Crystal shape	sphere	sphere	sphere	sphere	sphere
Radius of crystal (mm)	0.105	0.215	0.155	0.14	0.10
μ for Mo $K\alpha$ (mm ⁻¹)	14.54	1.150	2.160	1.098	8.340
μR for Mo $K\alpha$	1.53	0.25	0.33	0.15	0.84
Diffractometer	Syntex $P2_1$	Philips PW1100	Syntex $P2_1$	Syntex $P2_1$	Syntex $P2_1$
Radiation (kV, mA)	Mo $K\alpha$ (40, 20)	Mo $K\alpha$ (40, 20)	Mo $K\alpha$ (40, 15)	Mo $K\alpha$ (40, 20)	Mo $K\alpha$ (40, 20)
Monochromator	graphite	graphite	graphite	graphite	graphite
Collimator (mm ϕ)	1.15	0.8	1.15	1.15	1.15
Scan type	ω - 2θ	ω - 2θ	ω - 2θ	ω - 2θ	ω - 2θ
Scan speed (° in ω/s)					
minimum	0.015	0.05	0.010	0.0125	0.015
maximum	0.081	0.05	0.081	0.081	0.081
Number of scans	1	5	1	1	1
Scan width (° in ω) ($a + b \tan \theta$)	1.1, 0.4	1.4, 0.6	1.35, 0.4	1.08, 0.4	1.1, 0.4
Maximum value of 2θ (°)	157	135	134	134	134
Number of reflections measured	1569	3542	3511	3725	3310
Number of reflections used	74	3155	3142	3438	2088

* Sasaki (1976); space group *C2/c* has been confirmed after the examination of multiple diffraction.

† Fujino, Sasaki, Takéuchi & Sadanaga (1980).

Method I. Use of atomic scattering factors in different ionic states

Preliminary test

As a preliminary test to see the convergence of charge refinement, we studied, using the intensity data of Mn_2SiO_4 , the variation of the value of the residual factor, $\sum w_i (|F_{\text{obs}}| - |F_{\text{calc}}|)_i^2$, by calculating structure factors based on various arbitrarily assigned ionic states of Si and O. Fig. 1 shows the variations of the residual factors in various cases in each of which the charge of O was varied at intervals of 0.25 e while that of Si was given a fixed value; for each set of fixed charges of Si and O, the charges of Mn at the independent sites, $M(1)$ and $M(2)$, of Mn_2SiO_4 were refined, and the residual factors plotted for each of the different charges of Si were found to lie on a concave curve. When charges of O and Mn were refined with the charge of Si fixed, the resulting residual factor coincided with the minimum point of the above concave curve where the refined charges of $M(1)$ and $M(2)$ sites are given in parentheses in Fig. 1. When charges of all atoms were simultaneously refined, the residual factor converged to the position of 'convergence' in Fig. 1. Thus it was confirmed that the residual factor had only one minimum and the least-squares calculation for charge refinement is a valid procedure.

Procedure

Now, the atomic scattering factor f of an atom may be given by

$$f(s/2) = f_M(s/2) + pf_{m-M}(s/2) + f' + if'', \quad (1)$$

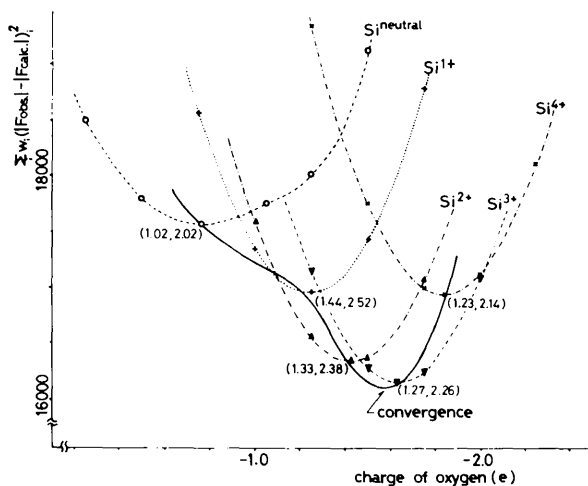


Fig. 1. Relationship between residual factors and f 's. Each broken or dotted curve shows the variation of residual factors when varying the charge of the O atoms with that of the Si atom fixed in Mn_2SiO_4 . The heavy line indicates the variation of converged residual factors when varying the charge of Si.

where $s = 2 \sin \theta/\lambda$, p is an occupancy factor to be determined, and f' and f'' are the terms of anomalous scattering. In this expression f_M represents f of the atom in an ionic state M , and f_{m-M} is given by the difference between f 's for two ionic states, m and M ; in this study m and M are assumed to have formal charges q and $q + 1$, respectively. This treatment was made because the variation of f versus q is not linear for a wide range of q (Fig. 2). This relation between f and q is such that, if a linear combination of f for core electrons (or fully ionized atom) and that for a neutral atom is used to determine the atomic charge, the resulting charge will be less ionic than the true one. When the parameter κ (Coppens *et al.*, 1979) is introduced, (1) is rewritten as

$$f(s/2) = f_{\text{core}}(s/2) + f_{M-\text{core}}(s/2\kappa) + pf_{m-M}(s/2\kappa) + f' + if''. \quad (2)$$

For calculations, the parameters p and κ were simultaneously refined with all other parameters. The refinement was made so as to minimize the residual factor $\sum w_i (|F_{\text{obs}}| - |F_{\text{calc}}|)_i^2$ with w_i unity. For (1) the least-squares program *EARTH* modified from *LINUS* (Coppens & Hamilton, 1970) was used, and for (2) *RADIEL* (Coppens *et al.*, 1979).

The difference of f 's between different ionic states is relatively conspicuous in the lower region of $\sin \theta/\lambda$. In the cases of MnO , Mn_2SiO_4 and $\text{LiAlSi}_2\text{O}_6$, however, the charge parameters refined with full data showed good agreement with those obtained with lower-order data sets ($\sin \theta/\lambda$ up to $0.5 \sim 0.8 \text{ \AA}^{-1}$).

All variables converged well after several cycles in each case. Although the correlation between scale and extinction factors in particular was relatively strong, their correlation coefficients were in the range 0.6 to 0.7. A few pairs of the parameters $p - \kappa$ and $\kappa - \beta_{ij}$ had coefficients ranging from 0.5 to 0.55. The rest were less than 0.5. The κ parameter can be applied only to atoms having valence electrons; for atoms having only a very small number of valence electrons, such as Li, Mg and Ca ions, the refinements did not converge. Therefore, the refinements using κ for those atoms could be performed under certain restricted conditions, *e.g.* κ was fixed at 1.0 or applied to some of the core electrons (Table 4). Final atomic parameters refined based on (1) are shown in Table 2,* while κ values for each atom obtained from (2) are shown in Table 3. In either case, the crystal charge was constrained to be neutral.

* Lists of structure factors and anisotropic thermal parameters have been deposited with the British Library Lending Division as Supplementary Publication No. SUP 35377 (69 pp.). Copies may be obtained through The Executive Secretary, International Union of Crystallography, 5 Abbey Square, Chester CH1 2HU, England.

Net atomic charges obtained in the final cycles of refinement are summarized in Table 4. The symbols $L1$ and $R1$ in the table indicate the values evaluated

respectively by (1) and (2), with the total charge in the crystal constrained to be zero, while $L2$ and $R2$ indicate the corresponding values when the constraint was released.

Method II. Calculation of the number of electrons within a sphere around an atom

Procedure

The number of electrons, $C(R)$, in a sphere of radius R around an atom can be obtained by using observed $F(hkl)$'s and correcting for termination effects. The derivation of $C(R)$ is given in Appendix A. The observed $F(hkl)$'s were obtained by using a relative scale factor in the process of charge refinement described before. Since the termination effect $\Delta C(R)$ is considered to be accurately corrected for by numerical integration in the Romberg method, a computer program designated *ENAC* was prepared by one of the authors (KF); after the correction the $C(R)$ curves increase gradually and smoothly against R . The procedure is described in Appendix B. Examples of $C(R)$ curves before and after termination corrections are shown in Fig. 3 for MnO and Mn_2SiO_4 ; full lines correspond to the values after the correction, while stars indicate the values from (A2). It must be mentioned that Kobayashi, Marumo & Saito (1972), to correct for termination errors, tried a method (a continual approximation) which is different from ours described above.

Table 2. Fractional atomic coordinates with e.s.d.'s in parentheses for MnO, $LiAlSi_2O_6$, $CaMgSi_2O_6$ and $Mg_2Si_2O_6$ after charge refinements $L1$

	x	y	z	B_{iso}^*	R
MnO					
Mn	0.0	0.0	0.0	0.617 (5)	0.0102
O	0.5	0.5	0.5	0.72 (1)	
$LiAlSi_2O_6$					
Al(M1)	0.0	0.90655 (2)	0.25	0.306	0.0152
Li(M2)	0.0	0.27609 (16)	0.25	1.176	
Si	0.29413 (1)	0.09342 (1)	0.25594 (2)	0.282	
O(O1)	0.10978 (2)	0.08230 (2)	0.14061 (4)	0.390	
O(O2)	0.36475 (3)	0.26695 (3)	0.30080 (5)	0.615	
O(O3)	0.35662 (2)	0.98701 (3)	0.05799 (4)	0.599	
$CaMgSi_2O_6$					
Mg(M1)	0.0	0.90774 (3)	0.25	0.389	0.0260
Ca(M2)	0.0	0.30122 (2)	0.25	0.648	
Si	0.28664 (2)	0.09315 (2)	0.22987 (3)	0.346	
O(O1)	0.11572 (4)	0.08719 (5)	0.14200 (8)	0.491	
O(O2)	0.36133 (5)	0.25005 (5)	0.31881 (9)	0.640	
O(O3)	0.35076 (4)	0.01767 (5)	-0.00429 (8)	0.546	
$Mg_2Si_2O_6$					
Mg(M1)	0.37582 (2)	0.65378 (4)	0.86596 (6)	0.407	0.0234
Mg(M2)	0.37677 (2)	0.48699 (4)	0.35897 (7)	0.547	
Si(TA)	0.27172 (1)	0.34162 (3)	0.05040 (4)	0.291	
Si(TB)	0.47357 (1)	0.33734 (3)	0.79827 (5)	0.286	
O(O1A)	0.18341 (3)	0.34003 (7)	0.03463 (11)	0.416	
O(O1B)	0.56238 (3)	0.34044 (7)	0.80003 (11)	0.425	
O(O2A)	0.31097 (3)	0.50228 (7)	0.04334 (12)	0.506	
O(O2B)	0.43280 (3)	0.48306 (7)	0.68928 (13)	0.511	
O(O3A)	0.30313 (3)	0.22261 (7)	-0.16814 (12)	0.497	
O(O3B)	0.44763 (3)	0.19507 (7)	0.60357 (12)	0.477	

* Equivalent isotropic temperature factors except in MnO.

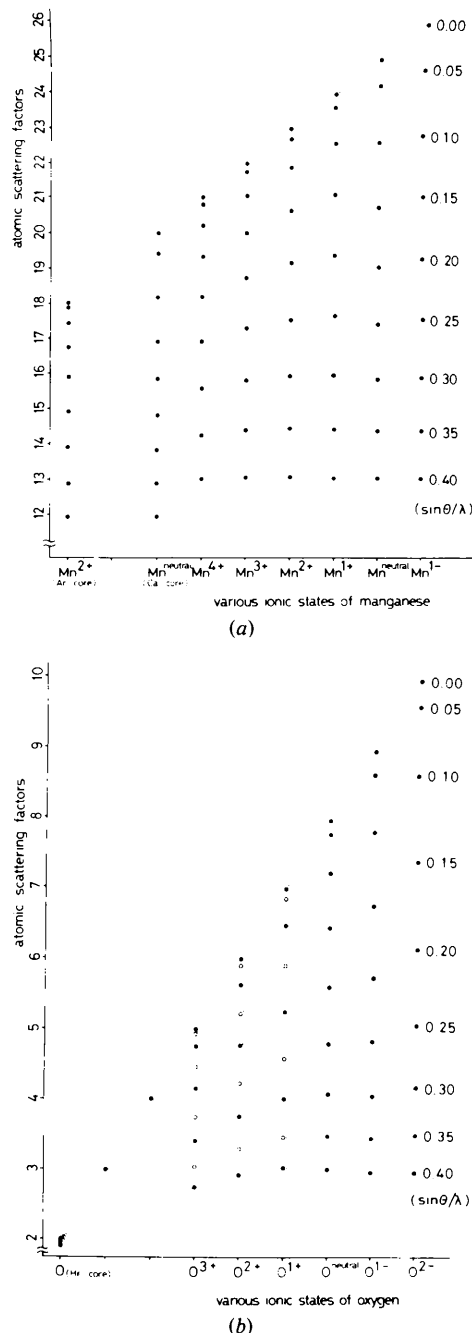


Fig. 2. Variation of the theoretical f'' of an atom with various ionic states of the atom; (a) Mn, (b) O. Each dotted line indicates f'' 's with the same $\sin \theta / \lambda$ value. The atomic scattering factors labelled as $Mn^{neutral}$ (Ca core) and Mn^{2+} (Ar core) correspond to Mn^{4+} and Mn^{7+} , respectively.

Table 3. Values of κ for each atom in five crystals after charge refinements R1

	M(1)	M(2)	Si	O(1)	O(2)	O(3)	
MnO	1.03 (5)			0.98 (1)			
Mn ₂ SiO ₄	0.99 (2)	0.99 (2)	1.05 (6)	1.01 (1)	1.02 (1)	1.01 (1)	
LiAlSi ₂ O ₆ *	1.255 (4)	0.92 (1)	1.00 (1)	1.001 (2)	1.004 (2)	1.008 (2)	
CaMgSi ₂ O ₆ *	0.981 (7)	1.100 (7)	1.07 (2)	1.009 (3)	1.007 (3)	1.018 (3)	
Mg ₂ Si ₂ O ₆ *	0.995 (3)	0.973 (4)	1.09 (2)	0.997 (3)	0.999 (4)	1.021 (4)	A site
			1.07 (3)	1.003 (4)	1.005 (4)	1.011 (4)	B site

* These κ values correspond to the R1* rows in Table 4.

Table 4. Atomic charges obtained from refinements using theoretical atomic scattering factors and total excess charges in a formula unit

The L- and R- rows give the values obtained from equations (1) and (2), respectively, while -1 and -2 rows represent those respectively with and without neutrality constraint.

The values in parentheses represent e.s.d.'s. For -1 rows of Mg₂Si₂O₆, $q(M1) = q(M2)$.

Crystal	Method	[M1]	[M2]	[Si]	[O1]	[O2]	[O3]	Excess charge	R				
MnO	(L1)	1.3(2)			-1.3()				1.02 %				
	(R1)	1.5(1)			-1.5()				1.03 %				
	(L2)	-0.1(12)			-2.2(8)			-2.3	1.02 %				
	(R2)	1.2(2)			-1.6(2)			-0.4	1.00 %				
Mn ₂ SiO ₄	(L1)	1.3(1)	2.2(2)	2.6(2)	-1.5(1)	-1.4(1)	-1.6()		3.10 %				
	(R1)	1.1(1)	2.1(2)	2.5(2)	-1.5(1)	-1.3(1)	-1.5()		3.09 %				
	(L2)	-0.2(2)	0.5(2)	1.6(2)	-2.1(1)	-1.9(1)	-2.2(1)	-6.6	3.10 %				
	(R2)	-0.4(2)	0.3(2)	1.7(3)	-2.1(3)	-1.9(2)	-2.3(1)	-6.9	3.08 %				
LiAlSi ₂ O ₆		[Al]	[Li]										
	(L1)	2.13(7)	3.3(2)	2.28(5)	-1.64(3)	-1.69(3)	-1.66()		1.52 %				
	(R1)***	2.28(6)	2.9(1)	2.29(5)	-1.65(3)	-1.65(3)	-1.59()		1.50 %				
	(R1)*	2.22(6)	3.3(2)	2.20(6)	-1.67(3)	-1.67(3)	-1.60()		1.48 %				
	(L2)	1.84(9)	0.7(3)	1.97(7)	-1.71(3)	-1.75(3)	-1.74(3)	-3.94	1.51 %				
	(R2)***	1.87(8)	0.1(3)	1.75(8)	-1.74(4)	-1.74(3)	-1.66(4)	-4.77	1.50 %				
CaMgSi ₂ O ₆		[Mg]	[Ca]										
	(L1)	2.7(2)	2.3(2)	2.57(7)	-1.71(5)	-1.64(5)	-1.73()		2.60 %				
	(R1)***	2.1(2)	2.7(2)	2.50(9)	-1.74(6)	-1.60(6)	-1.55()		2.54 %				
	(R1)*	2.5(2)	2.1(2)	2.62(8)	-1.75(6)	-1.63(5)	-1.55()		2.42 %				
	(R1)**	2.2(2)	2.6(2)	2.54(9)	-1.74(6)	-1.60(6)	-1.60()		2.54 %				
	(L2)	2.2(2)	1.0(5)	2.3(1)	-1.72(5)	-1.66(5)	-1.77(5)	-2.54	2.62 %				
Mg ₂ Si ₂ O ₆		[Mg]	[Mg]	[TA]	[TB]	[O1A]	[O1B]	[O2A]	[O2B]	[O3A]	[O3B]		
	(L1)	2.88()	2.88()	2.23(9)	2.52(9)	-1.94(6)	-1.76(5)	-1.74(6)	-1.83(6)	-1.68(6)	-1.56(6)	2.34 %	
	(R1)***	2.32()	2.32()	2.34(8)	2.55(8)	-1.76(6)	-1.58(6)	-1.60(6)	-1.62(6)	-1.51(6)	-1.48(6)	2.42 %	
	(R1)*	2.34()	2.34()	2.34(8)	2.53(8)	-1.76(6)	-1.58(6)	-1.61(6)	-1.63(6)	-1.50(6)	-1.47(6)	2.39 %	
	(L2)	0.7(1)	0.9()	1.4(1)	1.6(1)	-1.79(5)	-1.69(5)	-1.79(5)	-1.84(5)	-1.80(5)	-1.74(6)	-6.09	2.31 %
	(R2)***	0.8(1)	1.0(2)	1.5(1)	1.6(1)	-1.82(6)	-1.65(6)	-1.83(6)	-1.80(6)	-1.73(6)	-1.67(6)	-5.54	2.40 %
(R2)*	0.8(2)	1.0(2)	1.5(1)	1.6(1)	-1.81(6)	-1.65(6)	-1.82(6)	-1.80(6)	-1.71(6)	-1.67(6)	-5.58	2.36 %	

* κ was applied for 1s²2s¹ of Li, 2p⁶3s² of Mg and 3p⁶4s² of Ca.

** κ was applied for all electrons of Mg and Ca.

*** $\kappa = 1.0$ (fixed) for Li, Mg and Ca.

Although the values of $C(R)$ can be estimated with high accuracies, we must find a radius that may appropriately separate the atom from its neighbors. For this purpose we used the radial electron distribution, $U(R) = 4\pi R^2 \rho(R)$ and difference-Fourier maps; $U(R)$ was obtained by differentiating $C(R)$ with respect to R . We therefore prepared a program *POED* to calculate $U(R)$ and $dU(R)/dR$ from $C(R)$ and also to plot the resulting curves.

Characteristics of $U(R)$

Fig. 4 shows examples of $U(R)$ which we calculated with the above procedure for several atoms in MnO, LiAlSi₂O₆ and CaMgSi₂O₆. As observed in these figures, the $U(R)$ curve for a cation is characterized by a pair of peaks, the first peak being related to the electron density distribution of the cation and the second to the averaged electron density of neighboring

anions. The nearly flat region (*B* region) between these peaks sensibly varies from one bonding type to another. The $U(R)$ curves may then be classified into three types depending on the shape of the *B* region: (1) *minimum type*, (2) *flat type* and (3) *hump type*. The $U(R)$ curves such as those of Li and Mg have one minimum on the cation side of the *B* region in the *minimum type* (Fig. 4*b* and *c*). The minimum values of $U(R)$ for Li and Mg are 0.6 and 1.1 e/Å, respectively. Examples of the *flat type* characterized by a flat *B* region are given by Mn and Ca (Fig. 4*a* and *c*). The flat regions of Mn and Ca are within the radius 1.0 to 1.4 Å at the level of 3.3 e/Å and from 1.1 to 1.6 Å at 3.9 e/Å, respectively. Flat regions are also recognized with Co and Ni atoms in the NaCl-type mono-oxides (Sasaki *et al.*, 1979) and with Fe, Co and Ni in olivines (Fujino, Sasaki, Takeuchi & Sadanaga, 1980). The third type is specified by a small hump in the *B* region. For example, the $U(R)$ curve of Si in $\text{LiAlSi}_2\text{O}_6$ (Fig. 4*b*) has a small

hump at a distance of about 1.0 Å from the Si atom, the peak of the hump having a height of 11.3 e/Å.

Fig. 4 also shows the $U(R)$ curves of oxygen atoms, which have, within 1.2 Å from the center of the atom, two or more humps due to $1s^2$, $2s^2$ and so on. However, the details of the $U(R)$ curve depend upon the kinds of neighboring cation and the difference in coordination to cations.

Definition of atomic radius

In the radial distribution function, $U(R)$, of an atom, we can define the radius of the atom according to the above-mentioned types of $U(R)$ curve, and call the

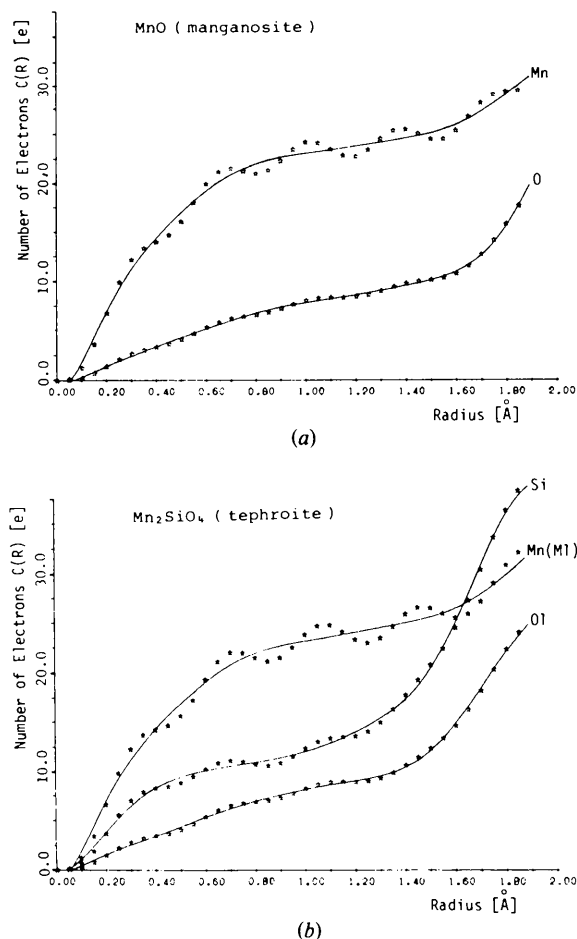


Fig. 3. Electron number $C(R)$ versus radius R . (a) Mn and O in MnO and (b) Mn, Si and O [O(1) site] in Mn_2SiO_4 . Curves shown by solid lines and stars are respectively after and before termination corrections.

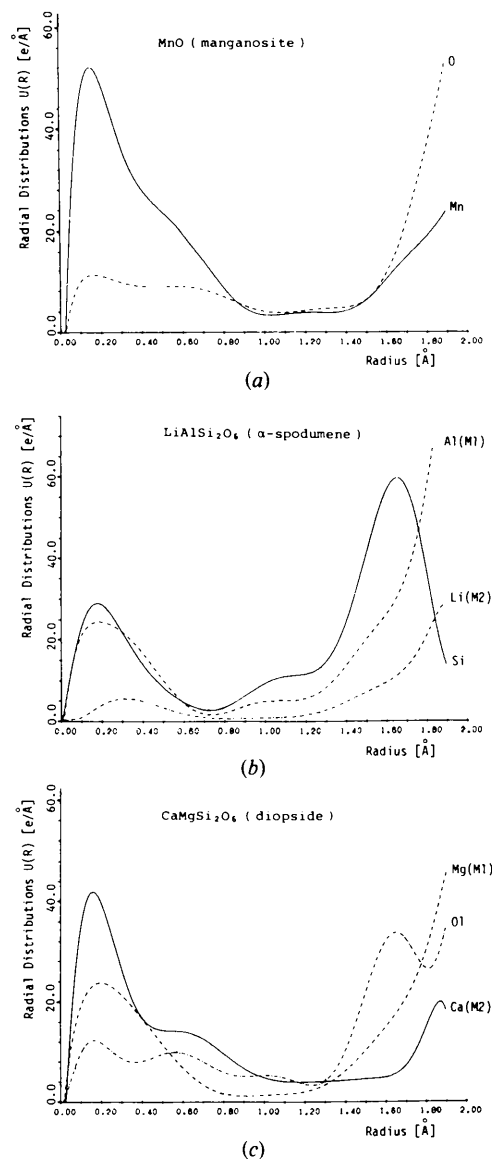


Fig. 4. Curves of $U(R)$ for (a) Mn and O in MnO , (b) Li, Al and Si in $\text{LiAlSi}_2\text{O}_6$ and (c) Ca, Mg and O [O(1) site] in $\text{CaMgSi}_2\text{O}_6$.

atomic radius thus defined the *effective (electron-density) distribution radius (ER)*.

(1) *Minimum type*. *ER* is defined as the distance from the cation to the minimum point of $U(R)$. The feature of the *B* region for Mg at the *M*(1) site in $\text{Mg}_2\text{Si}_2\text{O}_6$ is given in Table 5. For MgO (Sasaki *et al.*, 1979), the $U(R)$ of the oxygen atom also has a minimum at a point about 1.2 Å from the center. The sum of *ER* and the distance from oxygen to its minimum point is 2.12 Å, very close to the *M*–O distance, 2.11 Å. Thus the above definition of *ER* seems to be reasonable.

(2) *Flat type*. We propose to define *ER* by the relation

$$ER = (2R_m + R_{\text{oxy}})/3, \quad (3)$$

Table 5. Values of $C(R)$, $U(R)$ and $dU(R)/dR$ for Mg atom in the *M*(1) site of $\text{Mg}_2\text{Si}_2\text{O}_6$, and definition of radius *ER*

The regions 0.70–1.40 Å from Mg are shown at intervals of 0.02 Å. Ionic and crystal radii (+2, VI; Shannon, 1976) are 0.72 and 0.86 Å, respectively.

<i>R</i> (Å)	<i>C</i> (<i>R</i>) (e)	<i>U</i> (<i>R</i>) (e/Å)	$dU(R)/dR$ (e/Å ²)	Definition of <i>ER</i>
0.70	9.67	3.72	-21.8	
0.72	9.74	3.32	-17.9	
0.74	9.80	3.00	-14.4	
0.76	9.86	2.74	-11.3	
0.78	9.91	2.55	-8.5	
0.80	9.96	2.40	-6.1	
0.82	10.01	2.30	-4.2	
0.84	10.05	2.23	-2.6	
0.86	10.10	2.19	-1.4	
0.88	10.14	2.18	-0.4	
0.90	10.19	2.17	0.3	<i>ER</i> (= 0.89 Å)
0.92	10.23	2.18	0.8	
0.94	10.27	2.20	1.1	
0.96	10.32	2.23	1.4	
0.98	10.36	2.26	1.7	
1.00	10.41	2.30	2.1	
1.02	10.45	2.34	2.5	
1.04	10.50	2.40	3.0	
1.06	10.55	2.47	3.7	
1.08	10.60	2.55	4.6	
1.10	10.65	2.65	5.7	
1.12	10.71	2.78	6.9	
1.14	10.76	2.93	8.2	
1.16	10.82	3.11	9.7	
1.18	10.89	3.32	11.3	
1.20	10.96	3.56	12.9	
1.22	11.03	3.83	14.6	
1.24	11.11	4.14	16.3	
1.26	11.20	4.48	17.9	
1.28	11.29	4.86	19.5	
1.30	11.39	5.26	21.1	
1.32	11.50	5.70	22.5	
1.34	11.62	6.16	23.9	
1.36	11.75	6.65	25.2	
1.38	11.89	7.17	26.5	
1.40	12.03	7.71	27.7	

where R_m and R_{oxy} are radii which can be uniquely obtained by calculating $dU(R)/dR$. As shown in Fig. 5 for Mn in MnO, for example, R_m and R_{oxy} can be defined by the points having the averaged gradient of the *B* region of $U(R)$, which we find to be 1.75 e/Å^2 in this case. The averaged gradient was determined as the mean value of the maximum and minimum of $dU(R)/dR$ in the *B* region of $U(R)$. The numerical values of $dU(R)/dR$ for Mn in MnO are listed together with $C(R)$ and $U(R)$ in Table 6. The definition of *ER* as given by (3) seems to be plausible because of the following two points. Firstly, in the case of MnO, the sum of *ER* of Mn thus defined and the distance from the center of the oxygen atom to the minimum point of its $U(R)$ is nearly equal to the Mn–O distance. Coincidence like this was also found in the cases of CoO and NiO (Sasaki *et al.*, 1979). Secondly, for Mg and Li, both having $U(R)$ of the *minimum type*, the position with the minimum value of $U(R)$ is comparable to the radius derived from (3) by assuming, for the curves in Fig. 4, the *B* region as a flat region. In previous papers (Sasaki *et al.*, 1978, 1979), *ER* was defined as $(R_m + R_{\text{oxy}})/2$ for *flat type*, but *ER* of (3) is now considered to be better.

(3) *Hump type*. As will be discussed later, the position of the small hump in the $U(R)$ curve for Si corresponds to that of the positive peaks which often appear between Si and O in the difference-Fourier maps of well refined silicate structures. Since the values of $U(R)$ on both sides of the *B* region are remarkably

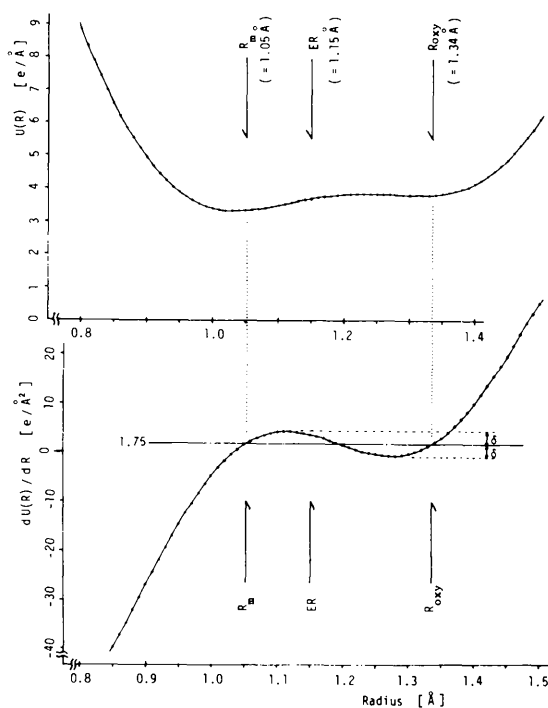


Fig. 5. Curves of $U(R)$ and $dU(R)/dR$ for the Mn atom in MnO.

different and the peaks of the difference-Fourier maps are thought to reflect the covalent character of Si—O bonds, we defined ER for Si by the average of the distances from Si to the four residual peaks in the maps which was found to be 0.96 Å in all $\text{LiAlSi}_2\text{O}_6$, $\text{CaMgSi}_2\text{O}_6$ and $\text{Mg}_2\text{Si}_2\text{O}_6$. The same length has been found in Mg_2SiO_4 (Fujino *et al.*, 1980).

(4) *Oxygen atom.* For oxygen atoms in NaCl-type mono-oxides it is possible to define ER at the minimum point of $U(R)$, but for those in silicates the $U(R)$ curve may not be made available for such a purpose because the oxygen atoms are coordinated by both octahedral and tetrahedral cations. Therefore, it is safe to estimate the atomic charge of oxygen with the aid of a neutrality constraint after having estimated the charges of cations in the crystal in terms of $C(ER)$.

Table 6. Values of $C(R)$, $U(R)$ and $dU(R)/dR$ for Mn atom in MnO, and definition of radii, R_m , R_{oxy} and ER

The regions 0.80–1.50 Å from Mn are shown at intervals of 0.02 Å. Ionic and crystal radii (+2, VI; Shannon, 1976) are 0.83 and 0.97 Å, respectively.

R (Å)	$C(R)$ (e)	$U(R)$ (e/Å)	$dU(R)/dR$ (e/Å ²)	Definition of radii
0.80	21.91	8.87	-50.4	
0.82	22.08	7.90	-46.5	
0.84	22.23	7.01	-42.1	
0.86	22.36	6.22	-37.3	
0.88	22.48	5.52	-32.2	
0.90	22.58	4.93	-27.1	
0.92	22.67	4.44	-22.0	
0.94	22.76	4.05	-17.1	
0.96	22.84	3.75	-12.6	
0.98	22.91	3.54	-8.5	
1.00	22.98	3.41	-4.9	
1.02	23.04	3.34	-1.9	
1.04	23.11	3.33	0.5	$R_m (=1.05 \text{ Å})$
1.06	23.18	3.36	2.3	
1.08	23.25	3.42	3.5	
1.10	23.32	3.49	4.1	
1.12	23.39	3.58	4.2	$ER (=1.15 \text{ Å})$
1.14	23.46	3.66	3.8	
1.16	23.53	3.73	3.2	
1.18	23.61	3.78	2.4	
1.20	23.68	3.82	1.4	
1.22	23.76	3.84	0.5	
1.24	23.84	3.84	-0.2	
1.26	23.91	3.83	-0.7	
1.28	23.99	3.82	-0.7	$R_{\text{oxy}} (=1.34 \text{ Å})$
1.30	24.07	3.81	-0.3	
1.32	24.14	3.81	0.6	
1.34	24.22	3.84	2.1	
1.36	24.30	3.90	4.2	
1.38	24.34	4.01	6.8	
1.40	24.46	4.17	10.0	
1.42	24.54	4.41	13.7	
1.44	24.63	4.72	17.7	
1.46	24.73	5.12	21.9	
1.48	24.84	5.60	26.3	
1.50	24.96	6.17	30.6	

Errors in $C(R)$

The estimation of errors in the calculation of $C(R)$ is presented in Appendix C and the magnitudes are shown in parentheses in Table 7, in which the values of R_m , R_{oxy} and ER are also listed together with respective $C(R)$'s. In Table 7, we compare the values of $C(R)$ based on ER with those defined by the middle point of the B region; the difference, Δ , is also given.

Discussion

Method I

The method involves inconsistency with chemically established facts as follows. (a) The total charge of every specimen examined has an excess negative charge when the neutrality constraint is released. In Table 4 this excess charge ranges from -1 to -7 e per chemical formula unit. (b) The atomic charge of a light atom such as Li and Mg with a neutrality constraint is inclined to show an excess positive value. In the $L1$ rows of Table 4, the charge of Li is $+3.3$ (2) e in $\text{LiAlSi}_2\text{O}_6$ and that of Mg is $+2.7$ (2) e in $\text{CaMgSi}_2\text{O}_6$ and $+2.9$ e in $\text{Mg}_2\text{Si}_2\text{O}_6$. (c) Mn atoms tend to have a negative charge when the neutrality constraint is released, the negative charge ranging from -1.0 to -0.4 e in $L2$ of MnO and $L2$ and $R2$ of Mn_2SiO_4 . (d) Li in the $R2$ rows is near neutral, $+0.1$ to $+0.2$ e.

Thus it seems to be hazardous to rely on the values of atomic charges obtained from (1) or (2). The above discrepancies are thought to be mainly due to the fact that the theoretical f in a free ionic state is unsuitable for the purpose of charge estimation in the crystalline state. The above examples show that the discrepancies were scarcely improved by introducing the κ parameters (Table 4).

On the other hand, for other purposes this method may be helpful. Refinements according to (1) or (2) significantly improved R values especially for crystals composed of light atoms. The R value of 0.0152 given by the refined f set of $\text{LiAlSi}_2\text{O}_6$ is clearly smaller than 0.0290 given by the neutral one or 0.0167 given by the fully ionized one. For $\text{CaMgSi}_2\text{O}_6$ these values are 0.0260, 0.0329 and 0.0267, respectively; for Mn_2SiO_4 0.0313, 0.0353 and 0.0313, respectively. Furthermore, calculated structure factors using charge-refined f values significantly improved difference-Fourier maps: ghost peaks otherwise occurring in the maps were mostly eliminated as will be shown later.

Method II

As shown in Table 7, the charge values obtained for cations are all less ionic than the corresponding formal charges and all more ionic than those in neutral states. Mg atoms are almost purely ionic except in

Table 7. Values of $C(R)$ for radii R_m , R_{oxy} and ER of Li, Mg, Al, Ca, Mn, Co and Ni atoms

$$\Delta = C(ER) - C(R'), R' = (R_m + R_{oxy})/2.$$

The error values in parentheses are different according to the type of four-circle diffractometer: in the Philips PW1100 the $\sigma F(hkl)$ includes the average error for strong reflections and an extra uncertainty about the background correction.

	Crystal	R_m (Å)	$C(R)$ (e)	R_{oxy} (Å)	$C(R)$ (e)	ER (Å)	$C(R)$ (e)	Charge (e)	Δ (e)
Li(M2)	LiAlSi ₂ O ₆					0.83	2.3 (1)	+0.7 (1)	0.1
Mg	MgO*					0.92	10.15 (0)	+1.85 (0)	0.13
(M1)	Mg ₂ Si ₂ O ₆					0.89	10.16 (4)	+1.84 (4)	0.14
(M2)	Mg ₂ Si ₂ O ₆					0.96	10.21 (4)	+1.79 (4)	0.07
(M1)	CaMgSi ₂ O ₆					0.91	10.56 (1)	+1.44 (1)	0.09
Al(M1)	LiAlSi ₂ O ₆	0.78	10.24 (8)	1.18	11.9 (2)	0.91	10.6 (1)	+2.4 (1)	0.2
Ca(M2)	CaMgSi ₂ O ₆	1.13	18.08 (2)	1.55	19.85 (3)	1.27	18.61 (2)	+1.39 (2)	0.30
Mn	MnO	1.05	23.14 (1)	1.34	24.22 (1)	1.15	23.49 (1)	+1.51 (1)	0.17
(M1)	Mn ₂ SiO ₄	1.05	23.35 (6)	1.34	24.66 (7)	1.15	23.79 (6)	+1.21 (6)	0.21
(M2)	Mn ₂ SiO ₄	1.06	23.16 (6)	1.35	24.21 (7)	1.16	23.51 (6)	+1.49 (6)	0.16
Co	CoO*	0.99	25.19 (1)	1.29	26.45 (1)	1.09	25.60 (1)	+1.40 (1)	0.24
Ni	NiO*	0.99	26.63 (1)	1.26	28.02 (1)	1.08	27.09 (1)	+0.91 (1)	0.23

* From Sasaki, Fujino & Takéuchi (1979).

Table 8. Final net atomic charges for each atom in MnO, Mn₂SiO₄, LiAlSi₂O₆, CaMgSi₂O₆ and Mg₂Si₂O₆

The values in parentheses represent the errors in the estimation of $C(R)$.

Crystal	M		Si		O(1)		O(2)		O(3)	
	$M(1)$	$M(2)$	TA	TB	O(1A)	O(1B)	O(2A)	O(2B)	O(3A)	O(3B)
MnO	+1.58 (1)									
Mn ₂ SiO ₄	+1.21 (6)	+1.49 (6)		+2.28 (5)		-1.27		-1.13		-1.29
LiAlSi ₂ O ₆	+2.4 (1)	+0.7 (1)		+2.4 (1)		-1.3		-1.4		-1.3
CaMgSi ₂ O ₆	+1.44 (1)	+1.39 (2)		+2.56 (1)		-1.33		-1.28		-1.35
Mg ₂ Si ₂ O ₆	+1.84 (4)	+1.79 (4)	+2.20 (4)	+2.36 (4)		-1.51 -1.37		-1.36 -1.43		-1.31 -1.22

CaMgSi₂O₆. The $M(1)$ site of CaMgSi₂O₆ may contain a minor amount of such an impure element as Fe. Moreover, Mg is more ionic than the transition metals such as Mn, Co and Ni. Si atoms in silicate, as given in Table 8, are less ionic than octahedral cations. The charge of an oxygen atom in a crystal ranges from -1.0 to -2.0 e. Note that this method bears no inconsistency with chemically established facts compared to the previous method I.

$U(R)$ and ER used to estimate the above charges are nearly identical for the same kinds of cation within experimental error, regardless of the difference in structure types. This means that ER is a measure of the practical radius for each atom in a crystal. Further details on experimental data will be reported in another paper which will mainly deal with olivine structures (Fujino *et al.*, 1980).

Difference-Fourier syntheses

Fig. 6 shows the difference-Fourier maps on the plane passing through Si-O(1) and Si-O(2) bonds in

LiAlSi₂O₆, which were synthesized using the difference $|F_{obs}| - |F_{calc}|$ obtained at the final steps of refinements with three different f sets: Fig. 6(a), (b) and (c) are the maps based on the structure factors calculated from neutral, fully ionized and charge-refined ($L1$) f 's, respectively. As seen in these maps with contour intervals of $0.1 \text{ e}/\text{Å}^3$, some ghost peaks in Fig. 6(a) and (b) are eliminated in Fig. 6(c). This effect seems to be significant in general when a crystal is composed mostly of light atoms.

After atomic charges were refined in $L1$, the difference-Fourier syntheses passing through the plane with two Si-O(3) bonds (bridging) were calculated and the map is plotted in Fig. 7. The four residual peaks in each of the Si tetrahedra thus observed are arranged at about 0.96 Å toward each oxygen from the central Si atom with peak heights of about $0.4 \text{ e}/\text{Å}^3$. Moreover, LiAlSi₂O₆ has negative peaks within the region up to about 0.5 Å , each from Si to the direction opposite to an oxygen atom. The location of residual peaks and the lesser ionicity of Si (see Table 8) suggest the existence of a σ bond between Si and O. Similar residual peaks

were found in $\text{CaMgSi}_2\text{O}_6$ and $\text{Mg}_2\text{Si}_2\text{O}_6$. A preliminary report on the residual peaks in $\text{LiAlSi}_2\text{O}_6$ has appeared (Fujino, Sasaki, Takéuchi & Sadanaga, 1976). These sorts of positive peak have also been reported for silicate spinels (Marumo, Isobe, Saito, Yagi & Akimoto, 1974; Marumo, Isobe & Akimoto, 1977) and pectolite (Takéuchi & Kudoh, 1977).

Summary

We conclude that the following procedure for charge determination will present the most plausible result for

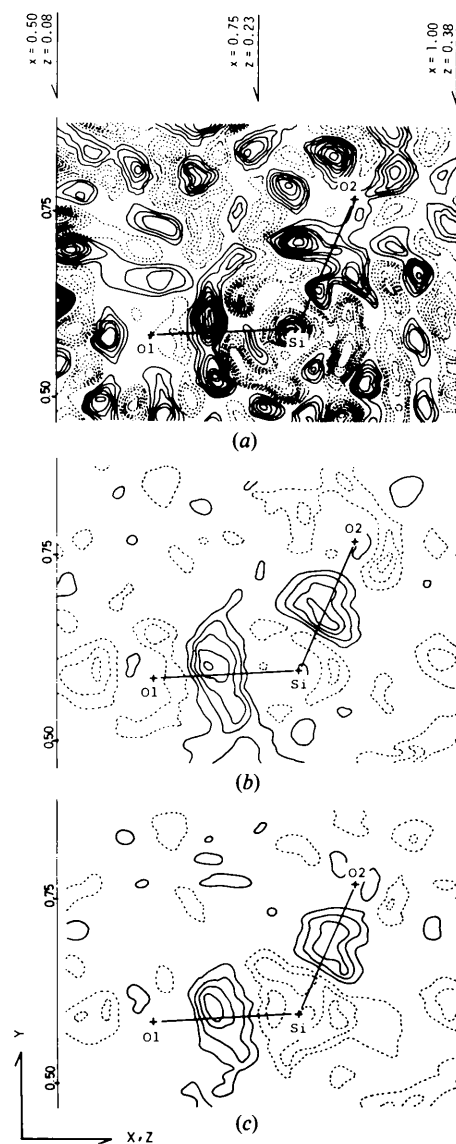


Fig. 6. Final difference-Fourier maps of $\text{LiAlSi}_2\text{O}_6$ using the following sets of f' 's: (a) neutral, (b) fully ionized and (c) charge refined (L1). Each shows a section passing through the O(1)–Si–O(2) bonds. Contours are at intervals of $0.1 \text{ e}/\text{Å}^3$; broken lines are negative contours, zero contours are omitted.

crystals of oxides and silicates. (1) For a cation exhibiting $U(R)$ of the *minimum* or *flat* type, its atomic charge should be derived from the number of electrons, $C(R)$, within the sphere of radius ER , which is defined by the radial distribution $U(R)$. (2) For Si, which exhibits $U(R)$ of the *hump* type, the charge is to be derived from $C(R)$ with ER (0.96 Å) which corresponds to the average of the distances from Si to the maxima of residual positive peaks occurring between Si and O atoms in the difference-Fourier maps. (3) After charges of cations in a crystal are determined with the above procedures, the charges of O atoms can be determined by refining the occupancy parameters, p , in (1) or (2), where the total charge of the crystal is constrained to be neutral.

The final atomic charges thus obtained are listed in Table 8. The charges of cations used here are less ionic than the corresponding formal ones. The charges of Si atoms are within the range from $+2.2$ to $+2.6 \text{ e}$ and those of O atoms from -1.1 to -1.5 e .

The authors are grateful to Drs S. Banno, J. Ito, K. Sakurai, Y. Sumino, H. Takei and K. Yokoyama for specimens. All computations were carried out on the HITAC 8800/8700 at the Computer Centre of the University of Tokyo.

APPENDIX A

Derivation of $C(R)$

The electron density at a point \mathbf{r} in a unit cell is given by

$$\rho(\mathbf{r}) = V^{-1} \sum_{hkl} \sum_{hkl} F(hkl) \exp(-2\pi i \mathbf{s} \cdot \mathbf{r}), \quad (\text{A1})$$

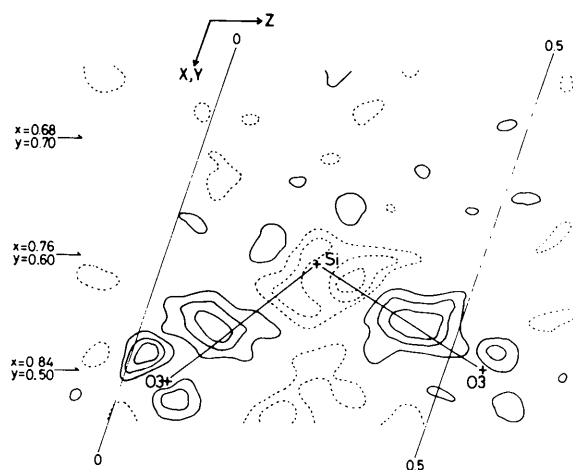


Fig. 7. Final difference-Fourier section passing through the O(3)–Si–O(3) bonds of $\text{LiAlSi}_2\text{O}_6$ after charge refinement (L1). Contours are at intervals of $0.1 \text{ e}/\text{Å}^3$; broken lines are negative contours, zero contours are omitted.

where $\mathbf{s} = h\mathbf{a}^* + k\mathbf{b}^* + l\mathbf{c}^*$. By integrating (A1), the number of electrons $C(R)$ in a sphere of radius R may be given by the formula

$$\begin{aligned} C(R) &= \int_{r < R} V^{-1} \left\{ \sum_{hkl} \sum F(hkl) \exp(-2\pi i \mathbf{s} \cdot \mathbf{r}) \right\} dV \\ &= V^{-1} \left\{ 4\pi R^3 F(000)/3 + (2\pi^2)^{-1} \right. \\ &\quad \times \sum_{hkl} \sum' [s^{-3} F(hkl) \exp(-2\pi i \mathbf{s} \cdot \mathbf{r}) \\ &\quad \times (-2\pi s R \cos 2\pi s R + \sin 2\pi s R)] \left. \right\}, \end{aligned} \quad (A2)$$

where $s = |\mathbf{s}| = 2 \sin \theta / \lambda$ and the observed $F(hkl)$'s are obtained after appropriate scaling during refinements. For unobserved reflections within the observation sphere as defined by radius s_{\max} , we used calculated $F(hkl)$'s (based on the final atomic parameters of charge refinements).

To correct for termination effects of the Fourier series, we must add the term $\Delta C(R)$ outside the observation sphere. Such a correction term may be given by replacing summations by integrals:

$$\begin{aligned} \Delta C(R) &= \int_{r < R} \left\{ \int_{s > s_{\max}} F_{\text{calc}}(hkl) \exp(-2\pi i \mathbf{s} \cdot \mathbf{r}) dV^* \right\} dV \\ &= \int_{s > s_{\max}} F_{\text{calc}}(hkl) \exp(-2\pi i \mathbf{s} \cdot \mathbf{r}) G(s, R) dV^*, \end{aligned} \quad (A3)$$

where

$$G(s, R) = (2\pi^2 s^3)^{-1} (-2\pi s R \cos 2\pi s R + \sin 2\pi s R)$$

and dV and dV^* are small volumes respectively in real and reciprocal spaces. To execute the integration, we adopt the analytical expression of atomic scattering factors given by Cromer & Mann (1968):

$$f(s) = \sum_{p=1}^4 a_p \exp(-b_p s^2/4) + c. \quad (A4)$$

Although the analytical form factors of Cromer & Mann lack accuracy at $\sin \theta / \lambda > 1.5 \text{ \AA}^{-1}$, the effect of the inaccuracy on the above treatment is negligible because the $C(R)$ curves obtained after the above termination correction are sufficiently smooth.

Using the isotropic temperature factor B_j , equation (A3) of the i th atom is then expressed by

$$\begin{aligned} \Delta C_i(R) &= \sum_{j=1}^{\text{NA}} m_j \sum_{p=1}^5 \alpha_p^j \int_{s_{\max}}^{\infty} \exp\{-s^2(b_p^j + B_j)/4\} \\ &\quad \times \left\{ \sum_{n=1}^{\text{NS}} \exp[2\pi i \mathbf{s} \cdot (\mathbf{r}_{jn} - \mathbf{r}_i)] G(s, R) \right\} dV^* \end{aligned}$$

$$\begin{aligned} &= \sum_{j=1}^{\text{NA}} m_j \sum_{p=1}^5 \alpha_p^j \sum_{n=1}^{\text{NS}} \int_{s_{\max}}^{\infty} \int_0^{\pi} \exp(2\pi i s r_{jni} \cos \theta) \\ &\quad \times \exp\{-s^2(b_p^j + B_j)/4\} \\ &\quad \times G(s, R) s d\theta ds (2\pi s \sin \theta), \end{aligned} \quad (A5)$$

where NA = number of atoms in an asymmetrical unit, NS = number of symmetry operations, m_j = multiplier for the j th atom, r_{jni} = distance between the i th atom and the atom given by the n th symmetry operation of the j th atom, $a_5 = c$ in (A4), $b_5 = \text{zero}$.

Let E and t/E respectively represent $(b_p^j + b_j)^{1/2}/2$ and s , then we obtain

$$\Delta C_i(R) = \sum_{j=1}^{\text{NA}} m_j \sum_{p=1}^5 \alpha_p^j \sum_{n=1}^{\text{NA}} Q, \quad (A6)$$

where

$$\begin{aligned} Q &= (E/r_{jni}\pi^2) \int_{Es_{\max}}^{\infty} t^{-2} \exp(-t^2) \sin(2\pi r_{jni} t/E) \\ &\quad \times [-(2\pi R t/E) \cos(2\pi R t/E) + \sin(2\pi R t/E)] dt \end{aligned}$$

and

$$\begin{aligned} Q &= 2/\pi \int_{Es_{\max}}^{\infty} t^{-1} \exp(-t^2) [-(2\pi R t/E) \cos(2\pi R t/E) \\ &\quad + \sin(2\pi R t/E)] dt \end{aligned}$$

respectively for $r_{jni} \neq 0$ and $r_{jni} = 0$.

APPENDIX B

Computation of $\Delta C(R)$

In practice, the integration in (A6) can be calculated with the Romberg method for the integral of the form

$$\int_{x_1}^{x_2} g(x) dx. \quad (B1)$$

After an Euler-Maclaurin summation and the trapezoidal rule, Romberg's table $T_{m,j}$ is generated as follows:

$$T_{m,j} = T_{m-1,j+1} + (T_{m-1,j+1} - T_{m-1,j})/4^{m-1}, \quad (B2)$$

where $i = 1, 2, 3, \dots, n$, n = the maximum number of division into subintegrals, $j = i - 1, i - 2, i - 3, \dots, 1$, $0, m = i - j - 1$.

Then the convergence criterion is

$$|T_{m-1,0} - T_{m,0}| = \text{EPS}/|x_2 - x_1|. \quad (B3)$$

In this study the EPS in (B3) had the appropriate values from 0.01 for MnO to 0.0001 for $\text{Mg}_2\text{Si}_2\text{O}_6$. This integration was computed up to the point $x_2 = 2.58$. In that case, the area of the integration,

$$\int_0^{x_2} \exp(-x^2) dx,$$

reaches 99.97% of the case in which the integration is calculated up to infinity. Test calculations using values larger than 2.58 gave a value of $C(R)$ which was the same as that of the $x_2 = 2.58$ case. In the HITAC 8800/8700 system, one atom in MnO and $Mg_2Si_2O_6$ requires 15 and 900 s of computation respectively to process 40 points of $C(R)$.

APPENDIX C

Estimation of errors via $C(R)$

The statistical error $\sigma C(R)$ of (A2) is evaluated from the standard deviation $\sigma F(hkl)$ of experimental structure factors:

$$\sigma C(R) = (2\pi^2 V)^{-1} \left\{ \sum \sum \sum [s^{-3} \sigma F(hkl) \times (-2\pi sR \cos 2\pi sR + \sin 2\pi sR)]^2 \right\}^{1/2}. \quad (C1)$$

Possible errors which may be caused by substituting summations for integrals were neglected. In the calculation of termination terms using the Romberg method, the uncertainty σT in (B2) is represented by

$$\sigma T = \left| \int_{x_1}^{x_2} g(x) dx - T_{m,j-1} \right| \\ = |(x_2 - x_1) N_{2j} 2^{-2mj} g^{(2j)}(\xi) / 2^{j(j-1)} (2j)!|. \quad (C2)$$

Here N_{2j} is a Bernoulli number, $N_2 = 1/6$, $N_4 = 1/30$, ..., and ξ is a point within a small interval. In general this quantum is smaller than $\sigma C(R)$ and is therefore negligible.

References

- BECKER, P. J. & COPPENS, P. (1974). *Acta Cryst.* **A30**, 129–147.
 COPPENS, P., GURU ROW, T. N., LEUNG, P., STEVENS, E. D., BECKER, P. J. & YANG, Y. W. (1979). *Acta Cryst.* **A35**, 63–72.

- COPPENS, P. & HAMILTON, W. C. (1970). *Acta Cryst.* **A26**, 71–83.
 COPPENS, P., PAUTLER, D. & GRIFFIN, J. E. (1971). *J. Am. Chem. Soc.* **93**, 1051–1058.
 CROMER, D. T. & MANN, J. B. (1968). *Acta Cryst.* **A24**, 321–324.
 FUJINO, K., SASAKI, S., TAKÉUCHI, Y. & SADANAGA, R. (1976). *Crystallogr. Soc. Jpn 1976 Annual Meeting*, Abstract p73.
 FUJINO, K., SASAKI, S., TAKÉUCHI, Y. & SADANAGA, R. (1980). In preparation.
 FUKAMACHI, T. (1971). *Tech. Rep. B12*, Inst. of Solid State Physics, Univ. Tokyo.
 HAVIGHURST, R. J. (1927). *Phys. Rev.* **29**, 1–19.
International Tables for X-ray Crystallography (1962). Vol. III. Birmingham: Kynoch Press.
International Tables for X-ray Crystallography (1974). Vol. IV. Birmingham: Kynoch Press.
 KOBAYASHI, A., MARUMO, F. & SAITO, Y. (1972). *Acta Cryst.* **B28**, 2709–2715.
 KURKI-SUONIO, K. & SALMO, P. (1971). *Ann. Acad. Sci. Fenn. Ser. A6*, No. 369.
 MARUMO, F., ISOBE, M. & AKIMOTO, S. (1977). *Acta Cryst.* **B33**, 713–716.
 MARUMO, F., ISOBE, M., SAITO, Y., YAGI, T. & AKIMOTO, S. (1974). *Acta Cryst.* **B30**, 1904–1906.
 SASAKI, S. (1976). MSc thesis submitted to Dept Earth Sciences, Kanazawa Univ.
 SASAKI, S., FUJINO, K. & TAKÉUCHI, Y. (1979). *Proc. Jpn Acad.* **55B**, 43–48.
 SASAKI, S., FUJINO, K., TAKÉUCHI, Y. & SADANAGA, R. (1977). *Crystallogr. Soc. Jpn 1977 Annual Meeting*, Abstract PB-2.
 SASAKI, S., FUJINO, K., TAKÉUCHI, Y. & SADANAGA, R. (1978). *Acta Cryst.* **A34**, S21.
 SHANNON, R. D. (1976). *Acta Cryst.* **A32**, 751–767.
 STEWART, R. F. (1970). *J. Chem. Phys.* **53**, 205–213.
 TAKÉUCHI, Y. & KUDOH, Y. (1977). *Z. Kristallogr.* **146**, 281–292.
 TOKONAMI, M. (1965). *Acta Cryst.* **19**, 486.
 VAHBASELKÄ, A. & KURKI-SUONIO, K. (1975). *Phys. Fenn.* **10**, 87–99.
 ZACHARIASEN, W. H. (1967). *Acta Cryst.* **23**, 558–564.